



The human DNA topoisomerase I mutant Gly717Asp: Higher religation rate is not always associated with camptothecin resistance[☆]



Zhenxing Wang^a, Ilda D'Annessa^b, Cinzia Tesaro^{b,1}, Alessio Ottaviani^b, Bini Chhetri Soren^b, Jagadish Babu Dasari^b, Beatrice Messina^b, Anil Thareparambil^b, Paola Fiorani^{b,c,*}

^a Movement System Injury and Repair Research Center, Xiangya Hospital, Central South University, Changsha, 410008, Hunan, China

^b Department of Biology, University of Rome Tor Vergata, Via Della Ricerca Scientifica 1, 00133, Rome, Italy

^c Institute of Translational Pharmacology, National Research Council, CNR, Via Del Fosso del Cavaliere 100, Rome, 00133, Italy

ABSTRACT

DNA topoisomerases are key enzyme responsible for modulating the topological state of the DNA by breaking and rejoining of DNA strand. Characterization of a Gly717Asp mutation in the human topoisomerase was performed using several catalytic assays. The mutant enzyme was shown to have comparable cleavage and fast religation rate as compared to the wild-type protein. Addition of the anticancer drug camptothecin significantly reduced the religation step. The simulative approaches and analysis of the cleavage/religation equilibrium indicate that the mutation is able to modify the architecture of the drug binding site, increasing the persistence of the drug for the enzyme–DNA covalent complex. Taken together these results indicate that the structure modification of the drug binding site is the key reason for the increasing CPT persistence and furthermore provide the possibility for new anti-cancer drug discovery.

1. Introduction

Human topoisomerase 1 (hTop1) enzyme is a ubiquitous and fundamental protein involved in cellular DNA processes such as replication, transcription, recombination and DNA repair [1,2]. The full length 765aa hTop1 is divided in four separate domains: the N-terminal domain (Met1–Gly214) is required for strand rotation, relaxation and subcellular localization of the enzyme *in vivo*; the highly conserved core domain (Ile215–Ala635) in which are present all the amino acids forming the catalytic pentad (Arg488, Lys532, Arg590, His632) except the active tyrosine (Tyr723); the linker domain (Pro636–Lys712), that plays an important role in the DNA cleavage/religation equilibrium, protrudes out of the enzyme by two opposite long α -helices; the C-terminal domain (Gln713–Phe765) is organized into five short α -helices, containing the active tyrosine (Tyr723) placed on the loop connecting α -helix20 to 21 [3–5]. The catalytic cycle of hTop1 is divided into five steps: 1) enzyme binding to the DNA; 2) cleavage of the DNA strand by the enzyme; 3) rotation of the DNA scissile-strand; 4) religation of the cleaved strand; 5) dissociation of the relaxed DNA. During these catalytic processes the enzyme goes through two different conformational changes: first, from an “open” structure that permits the binding of the DNA then to a “close” conformation. These finding was

observed by X-ray diffraction which shows that the enzyme completely embraces the DNA [6–8]. The enzyme relaxation activity has been proposed to occur through the “rotation model”, in which the enzyme changes the linking number of DNA allowing the free 5'-DNA substrate to rotate around the intact strand [9]. This rotation could be partially controlled by the linker domain, that acts as a ‘brake’ during the relaxation of the DNA, and by the V-shaped helices (in the core domain) via electrostatic interactions between the positive charged protein domains and the negative charged DNA [10]. HTop1 is of significant and important medical interest as it is the lone target of anticancer drugs such as camptothecin (CPT) and its water-soluble derivatives [11–13]. CPT is an alkaloid derived from a plant that blocks the synthesis of both DNA and RNA by binding explicitly and reversibly to the covalent enzyme-DNA complex thereby inhibiting the religation step of the catalytic cycle [14]. Stalled hTop1 can be converted into DNA strands breaks and the collision with replication fork leads to cell death [15]. Derivatives of CPT such as irinotecan and topotecan are used worldwide for various cancer treatments [16,17]. A major limitation for the successful cancer treatment with this drug is the acquired drug resistance which can arise due to several reasons, one of which is point mutations responsible for making hTop1 resistant to the drug [18]. Different mutations that affect the enzyme reactivity to CPT have been

[☆] This work was financially supported by Human Province Natural Science Foundation of China (Grant No. 2017JJ3501), China Postdoctoral Foundation (Grant No. 2017M612596) and a scholarship to Dr. Zhenxing Wang from Erasmus Mundus Action 2 TECHNO project.

* Corresponding author. Institute of Translational Pharmacology, National Research Council, Via Del Fosso del Cavaliere 100, 00133, Rome, Italy.
E-mail address: paola.fiorani@uniroma2.it (P. Fiorani).

¹ Present address: Department of Molecular Biology and Genetics, University of Aarhus, C.F Møllers Allè 3, 8000, Aarhus C, Denmark.

found situated in the drug binding site and in the linker domain. The movement of the linker domain has been shown to control the religation step affecting CPT sensitivity [4], particularly replacement of Ala to Pro at position 653 has been shown to render the enzyme resistant towards CPT. The Ala653Pro mutant confers an enhanced linker flexibility that is correlated with an increased religation kinetics that does not allow the CPT to stabilize the enzyme–DNA covalent complex [19]. On the other hand the double mutant Asp677Gly-Val703Ile shows hypersensitive to CPT and lower religation rate, correlated to a reduced linker flexibility [20]. The Lys681Ala mutant is also located in the linker domain, displays a reduced religation rate due to the perturbed linker dynamics, without affecting drug reactivity [21]. Finally the Glu710Gly show altered CPT reactivity by affecting the active site arrangement and linker flexibility [22]. These findings show that the linker domain and the active site of the protein are able to communicate in order that a mutation on the linker may affect the active site. It has been previously reported by our group that Gly717Phe mutant leads to drug resistance *in vivo* and was shown to have a faster religation rate that is partially reduced in the presence of the CPT [23]. The same mutation has been also reported by Van der Merwe and Bjornsti, in which the Gly721 in the yeast enzyme, corresponding to the human Gly717, gives rise to a CPT resistant mutant. In the same work it has been also reported the substitution of Gly721 with Asp that increases the CPT sensitivity, likely due to a conformational change within the Top1 catalytic pocket [24,25]. Based on this evidence we decided to investigate, through a combined experimental and simulative approaches, the same mutation in hTop1 in which the homologous residue Gly717 was mutated in Asp. This mutant has a peculiar behaviour when compared to wild type, showing a fast religation rate that is significantly reduced in presence of CPT. Analysis of the cleavage/religation equilibrium indicates that the mutation is able to modify the drug binding site and to increase the persistence of the drug for the enzyme–DNA covalent complex. Molecular docking strengthens this data indicating that the mutation is able to modify the architecture of the binding site increasing the persistence of the drug for the binding pocket.

2. Materials and methods

2.1. Chemicals, yeast strains and plasmids

Camptothecin (CPT) was purchased from Sigma-Aldrich and was dissolved in 99.9% of dimethyl sulfoxide (DMSO) to a final concentration of 4 mg/ml (11.5 mM) and stored at -20°C until use. *Saccharomyces cerevisiae* Top1 null strain EK3 (*MATa*, *ura3-52*, *his3Δ200*, *leu2Δ1*, *trp1Δ63*, *Top1::TRP1*) was used to express the hTop1 gene and test the sensitivity of the drug *in vivo*. To express the hTop1 under the galactose-inducible promoter a single copy plasmid YCpGAL1-e-hTop1 was adopted [26]. The epitope-tag FLAG (DYKDDDDY, indicated with ‘e’) was subcloned into YCpGAL1-hTop1 to produce the construct YCpGAL1-e-hTop1 containing the N-terminal sequence FLAG, recognized by the M2 monoclonal antibody. The mutant hTop1Gly717Asp was generated by using oligonucleotide-directed mutagenesis of the YCpGAL1-e-hTop1 as previously described [26].

2.2. Drug sensitivity assay *in vivo*

Cultures of yeast EK3 transformed with hTop1 wild type, hTop1 Gly717Asp mutation and vector were grown at an A_{595} of 0.3, and serially 10-fold diluted and 5 μl was spotted onto selective media containing dextrose or galactose. CPT sensitivity was assayed on galactose plates containing 25 mM HEPES (pH 7.2) and the indicated concentrations of CPT. Plates were incubated at 30°C for 3 days.

2.3. Enzyme purification

EK3 yeast cells were transformed with the hTop1 and Gly717Asp expression vector. The cells were grown on SC-uracil plus 2% dextrose overnight. At an optical density A_{595} of 1.0 they were diluted 1:100 in SC-uracil containing 2% raffinose. The cells were then induced with 2% galactose for 6 h. The cells were then harvested as described [27]. The extracts of hTop1 and Gly717Asp were applied to an anti-FLAG M2 affinity gel. Columns were then washed according to the manufactured protocol (Sigma Aldrich). The protein was eluted by adding five column volumes of a solution containing 1 mg of FLAG peptide in TBS. Protein levels and integrity were assessed by immunoblot with the monoclonal anti-M2 antibody. Similar concentrated fractions of hTop1 and Gly717Asp mutant were compared to the purified hTop1 with a known concentration (provided from Topogen) by immunoblot using the ab58313 Anti-hTop1B antibody (Abcam) and ab97240 goat polyclonal secondary antibody (Abcam). The *in vitro* experiments have been performed using an equal amount of purified hTop1 and Gly717Asp mutant [28].

2.4. Cleavage kinetics

The oligonucleotide CL14-U (5'-GAAAAAAGACTUAG-3') containing an hTop1 high-affinity cleavage site, was 5'-end labeled with [γ 32P] ATP. The CP25 complementary strand (5'-TAAAAATTTTCTAAGTCTTTTTC-3') was 5'-end phosphorylated with unlabeled ATP. The two strands were annealed with a 2-fold molar excess of CP25 over CL14U to produce the suicide substrate and the experiments were performed as described [29]. The percentage of the cleaved substrate (Cl1) was determined by PhosphorImager and ImageQuant software and normalized to the total amount of radioactivity in each lane.

2.5. Religation kinetics

The oligonucleotide CL14 (5'-GAAAAAAGACTTAG-3) containing an hTop1 high-affinity cleavage site was 5'-end labeled with [γ 32P] ATP. The CP25 complementary strand (5'-TAAAAATTTTCTAAGTCTTTTTC-3') was 5'-end phosphorylated with unlabeled ATP. The two strands were annealed with a 2-fold molar excess of CP25 over CL14 to produce the suicide substrate. 20 nM of CL14/CP25 was incubated with an excess of hTop1 or equal amount of Gly717Asp mutant for 60 min at 25°C followed by 30 min at 37°C in 20 mM Tris-HCl pH 7.5, 0.1 mM Na_2EDTA , 10 mM MgCl_2 , 50 $\mu\text{g}/\text{ml}$ acetylated BSA, and 150 mM KCl. After the formation of the cleavage complex (Cl1) a 5 μl aliquot was removed and used as time 0 point, then DMSO or 100 μM CPT were added and religation reaction was started by adding a 200-fold molar excess of R11 oligonucleotide (5'-AGAAAAATTTT-3') over the CL14/CP25. 5 μl aliquots were removed at various time points, and the reaction stopped with 0.5% SDS. After ethanol precipitation, samples were resuspended in 5 μl of 1 mg/ml trypsin and incubated at 37°C for 60 min. A trypsin resistant peptide remains attached to the substrate causing the 12 nt (Cl1) oligonucleotide to run slower than the uncleaved oligonucleotide in the gel [25]. Samples were analyzed by denaturing 7 M urea/20% polyacrylamide gel electrophoresis. The percentage of residual cleavage complex was quantified by ImageQuant software, normalized to the total radioactivity for each lane and to the value at $t = 0$ and finally plotted as a function of time.

2.6. Cleavage/religation equilibrium

Oligonucleotide CL25 (5'-GAAAAAAGACTTAGAAAAATTTTA-3') has been radiolabeled with [γ 32P] ATP at its 5'-end. The CP25 complementary strand (5'-TAAAAATTTTCTAAGTCTTTTTC-3') was phosphorylated at its 5'-end with unlabeled ATP. The two strands were annealed at a 2-fold molar excess of CP25 over CL25. A final concentration of 20 nM duplex CL25/CP25 was incubated with an excess of

the enzyme at 25 °C in 20 mM Tris-HCl pH 7.5, 0.1 mM Na₂EDTA, 10 mM MgCl₂, 50 mg/ml acetylated BSA, and 150 mM KCl, in the presence of the indicated concentration of CPT. The samples were stopped at the indicated time points by 0.5% SDS, digested with trypsin after ethanol precipitation and reactions were resolved in 20% polyacrylamide-7M urea gels.

2.7. Limited proteolysis

An equal amount of wild-type or Gly717Asp mutant was digested for 30 min at 37 °C with increasing concentrations of trypsin in 100 mM KCl, 1 mM EDTA and 1 mM DTT standard digestion buffer [5]. The reactions were stopped by SDS protein-dye and fractionated by SDS-PAGE, visualized by immunoblot using the ab58313 Anti-hTop1B antibody (Abcam) and ab97240 goat polyclonal secondary antibody (Abcam).

2.8. Computational methods

The starting coordinates for the protein and the 22 DNA bp forming the hTop1B-DNA covalent complex have been derived as described in Mancini et al., 2010 [29]. The Gly717Asp mutation has been introduced with the leap program of Amber directly upon topology building. The atom force field in Amber10 was used with parmbsc0 force field corrections. Each complex was immersed in a rectangular box and then solvated with TIP3P water molecules, and later neutralized by adding Na⁺ counter-ions. The simulations were run with the GROMACS MD package version 4.5.3 [30]. The electrostatic interactions were taken into consideration by means of the Particle Mesh Ewald method (PME) with a cut off of 1.2 nm for the real space and Van der Waals interactions [31]. LINCS algorithm was used to constraint all the bond lengths and angles [32]. Relaxation of solvent molecules and Na⁺ ions was initially performed with subsequent steps of 200 ps at 50, 100, 150, 200, 250 K till a final temperature of 300 K. The two systems were then simulated for 75ns using a time step of 2.0 fs and the neighbor list was updated after every 10 steps. The temperature was maintained constant at 300 K by using the velocity rescale using a coupling constant of 0.1 ps during the time of sampling, and the pressure was maintained at 1 bar using the Parrinello-Rahman barostat with a coupling constant of 1.0 ps during sampling [33]. Docking predictions were performed with Autodock4.2 [34] after preparation of the ligand and receptor structures using the AutodockTools suite v. 1.5.6 [34]. 250 docking runs were performed for each experiment using the Lamarckian Genetic Algorithm in order to generate the docked complex [35].

3. Results

3.1. Drug sensitivity assay

The human Gly717Asp mutant has been introduced in the single copy yeast plasmid (YCp) expressing the hTop1 under the GAL1 promoter. To assess the *in vivo* consequences of mutant expression, the viability and CPT sensitivity of Top1Δ yeast cells (EKY3), transformed with GAL1-hTop1 and Gal1-hTop1Gly717Asp have been tested. Serial dilutions of each transformed yeast cell were spotted on plates containing dextrose and galactose supplemented with different CPT concentrations, to assess drug sensitivity following the yeast growth. The data show that yeast cells, expressing the wild-type protein, exhibit a deficiency in viability in the presence of 10 ng/ml CPT as well as the Gly717Asp (Fig. 1).

3.2. Cleavage kinetics of the wild-type and Gly717Asp mutant

The cleavage kinetics has been carried out for the wild-type and Gly717Asp mutant in presence of a suicide cleavage substrate as

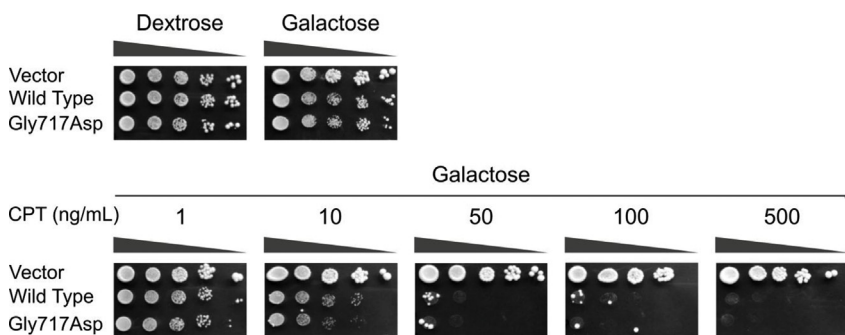
previously described [23]. A 5'-end radiolabeled oligonucleotide namely CL14-U having a ribo-Uracil (rU) in position 12 was annealed to complementary strand CP25 in order to produce a duplex having an 11-base 5'-single-strand extension, as shown in the top of Fig. 2A. After the enzyme nicks the substrate at the preferential binding site, 2'-OH ribose attacks the 3'-phosphotyrosyl linkage presents in between the enzyme and ribonucleotide, leading to enzyme release there by leaving a 2', 3'-cyclic phosphate. The reaction was carried out incubating the substrate with wild-type and mutant enzymes. The products were analyzed by denaturing urea polyacrylamide gel (Fig. 2A). After gel quantification the cleavage percentage, plotted as a function of time, indicates that the wild-type and the Gly717Asp have the same cleavage rate and reach a similar plateau value (Fig. 2B).

3.3. Religation kinetics of the hTop1 and Gly717Asp mutant

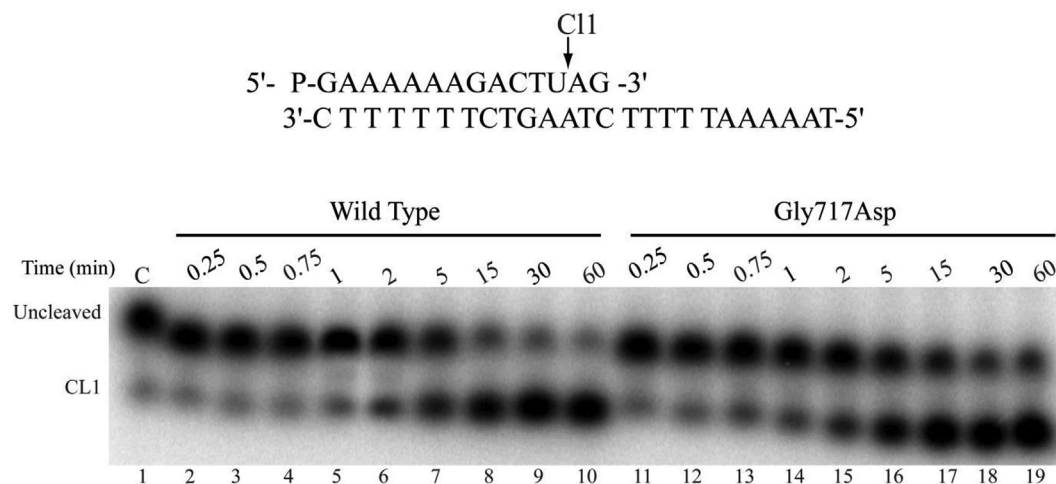
The DNA religation step has been studied by testing the ability of both enzymes to religate the oligonucleotide R11 (5'-AGAAAAAT TTT-3') in the presence and absence of CPT, which is added to the cleavage complex obtained by incubating the suicide substrate (CL14) with an excess of enzyme. Using this substrate, the religation step is almost totally precluded, because the AG-3' is too short to be religated, leaving the enzyme covalently attached to the 12 oligonucleotide 3'-end. Once Cleavage has occurred a 200-fold molar excess of complementary R11 oligonucleotide (5'-AGAAAAATTTT-3') has been added in the absence and presence of CPT. Aliquots have been removed at different times, the reaction stopped by addition of SDS and the products analyzed by polyacrylamide gel (Fig. 3A). The percentage of the remaining cleavage complex (Cl1) has been quantified as a function of time and plotted as shown in Fig. 3B. The data show that the Gly717Asp mutant (gray square full line) has a religation kinetics faster than the wild-type protein (black circle full line). Addition of CPT strongly inhibits the religation of the mutant (gray square dashed line) to a value comparable to that of the wild-type enzyme (black circle dashed line).

3.4. Cleavage/religation equilibrium in presence of CPT

The cleavage/religation equilibrium has been studied, analyzing the stability of the covalent DNA–enzyme complex using a full duplex oligonucleotide substrate CL25 (5'-GAAAAAGACTTAGAGAAAAAT TTT-3')/CP25 with increasing CPT concentrations (Fig. 4A). When both enzymes are incubated with DMSO, a small level of the cleaved substrate is detected at the preferred DNA cleavage site for both the wild type and the mutated enzyme (lanes 2 and 8). When CPT concentrations are increased, an enhancement of cleaved DNA substrate is observed (Fig. 4A, lanes 3–7), indicating that the equilibrium is shifted towards cleavage. The CPT incubation with the Gly717Asp mutant increases the amount of the covalent DNA–enzyme complex compared to the wild-type counterpart (Fig. 4A), compare lanes 3–6 with lanes 10–12) suggesting a stronger drug persistence for the mutated site. Comparative time-dependent cleavage/religation equilibrium has been performed for the two proteins in the absence and presence of 100 μM CPT. At different time points aliquots have been removed and analyzed on the urea-polyacrylamide gel (Fig. 4B). In the absence of CPT the Gly717Asp mutant shows a religation higher than the wild-type protein as evident from the intensity of the band in lanes 11–13 (Fig. 4B) which is lower than lanes 2–4 (Fig. 4B). When the wild-type protein is exposed to CPT, the equilibrium is strongly shifted toward cleavage as indicated by the increase of the intensity of the bands (Fig. 4B, lanes 5 to 10). The same occurs for the Gly717Asp mutant but to a greater extent (Fig. 4B, compare lanes 14–19 to lanes 5–10). These results confirm that CPT strongly persists on the mutant likely due to a low dissociation rate of the drug from the mutant cleavable complex.



A



B

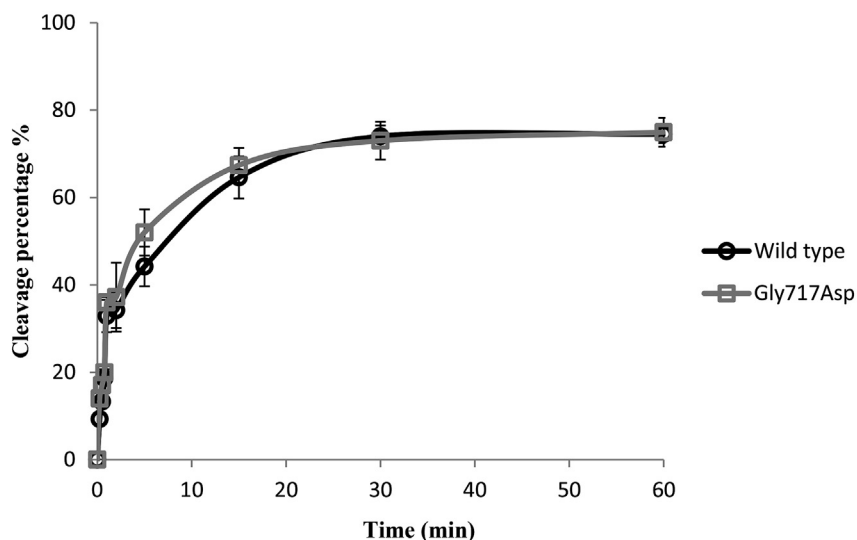
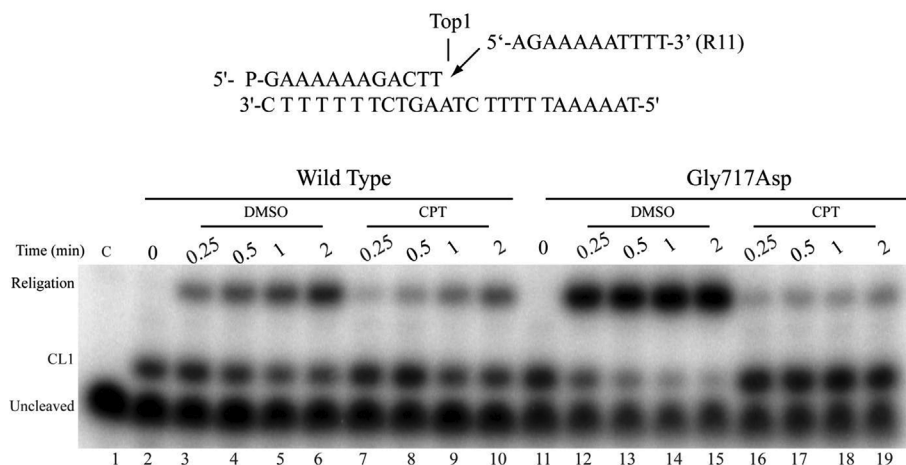
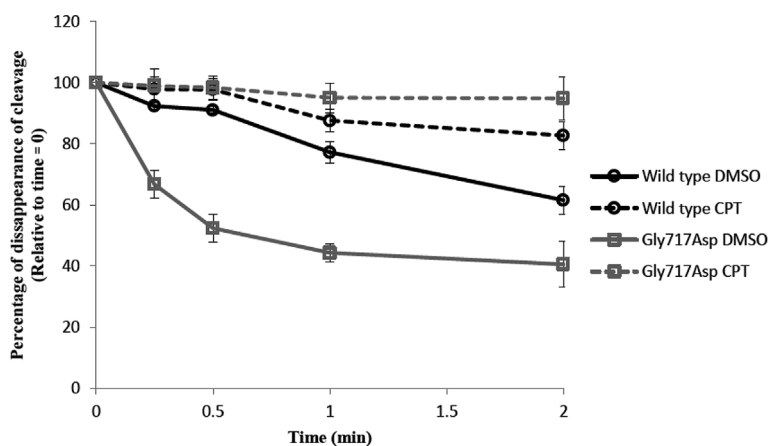


Fig. 2. Cleavage kinetics. (A) Time course of the cleavage reaction of wild-type (lanes 2–10) and Gly717Asp mutant (lanes 11–19) preformed with the CL14-U/CP25 substrate reported at the top of the figure. C, no protein added (lane 1). ClI identifies the cleaved strand by the enzymes at the preferred cleavage site. (B) Percentage of the cleaved fragment was plotted in function of time for wild-type (black dots) or the Gly717Asp mutant (gray squares). Three experiments were performed to obtain the average value and the standard deviation for error bars.

A



B



3.5. Evaluation of the CPT binding energy through docking studies

We have performed docking experiments in order to detect the binding energy of the compound for the wild-type and mutated covalent complex to obtain clues on the resting time of CPT in the two systems. Docking predictions, carried out using the X-ray structure of the wild-type enzyme, show that in all the resulting complexes the compound intercalates between the DNA bases as observed in the crystal structure and establishes interactions with residues Asp533 and Thr718; with a binding energy of about -10 kcal/mol. The calculation performed upon mutation of Gly717 in aspartic acid indicates a comparable binding energy of -10 kcal/mol. To better detect the effect of the mutation on the dynamics of the protein and on the CPT binding we have run an MD simulations of the wild-type and mutated covalent complex and repeated the docking experiment using as receptor the structures obtained after 75 ns of simulation time. In this case the docking results differ significantly. In the case of the wild-type, we

obtain three different families of structures, the most representative one having a CPT binding energy ranging between -9 and -8 kcal/mol. Interestingly, in this cluster of structures the CPT drug is oriented in a conformation different from the one observed in the X-ray structure (Fig. 5A and B). On the other hand, the mutant displays a unique binding site for CPT that interacts with the complex with a binding energy of -9 kcal/mol and with an orientation similar to the one observed in the X-ray structure of the wild type (Fig. 5B and C). These data suggest that the mutation is able to modify the architecture of the CPT binding site producing a pocket with a more negative binding energy. This result is in line with the increased persistence of CPT in the mutated cleavage complex, experimentally observed (Fig. 4).

3.6. Limited proteolysis of Top1

To investigate the previous hypothesis we have performed a limited proteolysis experiment that can be used to detect the conformational

Fig. 3. Religation kinetics. (A) Religation experiment of R11 complementary substrate (shown at the top of the figure) performed with the wild-type or Gly717Asp in absence (lanes 3–6 and lanes 12–15 for wild-type and Gly717Asp mutant respectively) or in the presence of $100 \mu\text{M}$ CPT (lanes 7–10 for the wild-type and lanes 16–19 for Gly717Asp mutant) in a time course dependent manner. C, no protein added (lane 1). Time 0 represents the completely cleaved substrate for the wild-type (lane 2) and the Gly717Asp mutant (lane 11). (B) The cleaved fragment, normalized to the time 0, plotted in function of time for the wild type in the presence of DMSO (full black line) or CPT (dashed black line) and for the Gly717Asp mutant in the presence of DMSO (full gray line) or CPT (dashed gray line). The error bars are the average of three independent experiments.

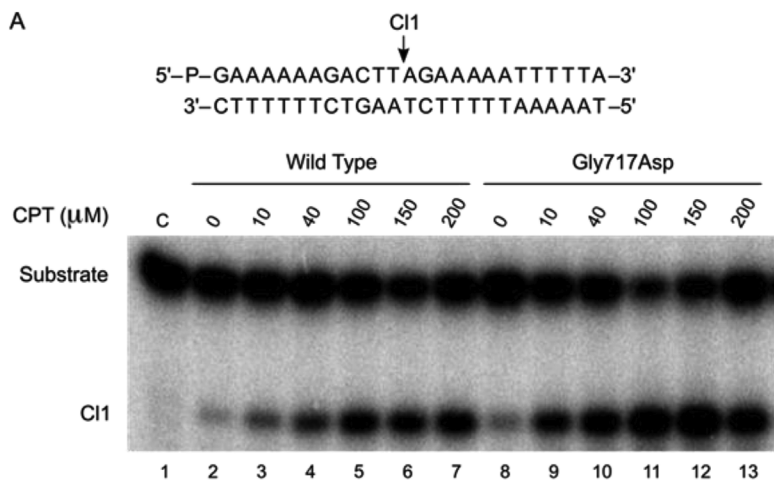


Fig. 4. Cleavage/religation equilibrium. (A) Gel electrophoresis of the products after incubation of the wild-type or Gly717Asp mutant proteins with radiolabeled duplex DNA, shown at the top of the figure, in the presence of an indicated amount of CPT. The arrow at the DNA sequence indicates the C1 preferred cleavage site. Lanes 2–7 (wild-type), lanes 8–13 (Gly717Asp). C, no protein added (lane 1). (B) Kinetics of the cleavage/religation equilibrium of wild-type and Gly717Asp mutant incubated with radiolabeled duplex DNA (shown at the top of the figure) in the absence (lanes 2–4 and lanes 11–13 for wild-type and Gly717Asp mutant respectively) or in the presence of 100 μM CPT (lanes 5–10 for the wild-type and lanes 14–19 for Gly717Asp mutant).

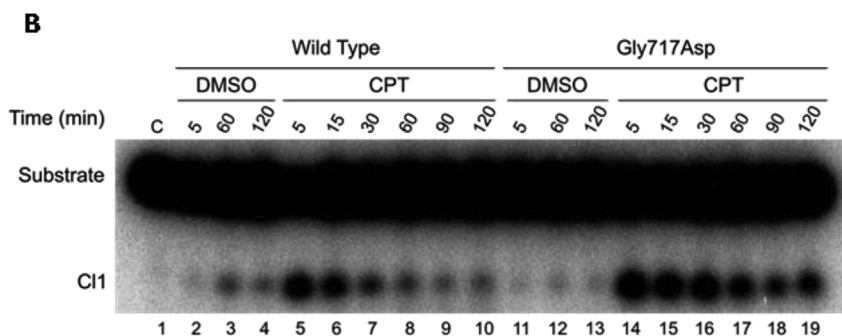


Fig. 5. Prediction of CPT binding mode after 75ns of simulation time. (A) A representative structure of the most populated family of docked complexes for the wild-type, (B) X-ray structure of the Topo1-DNA-CPT ternary complex (PDB code 1T81) and (C) Representative structure of the unique family of docked complexes for the mutant. In all the three panels the protein is shown in silver ribbon, the DNA in black and the CPT I grey stick.

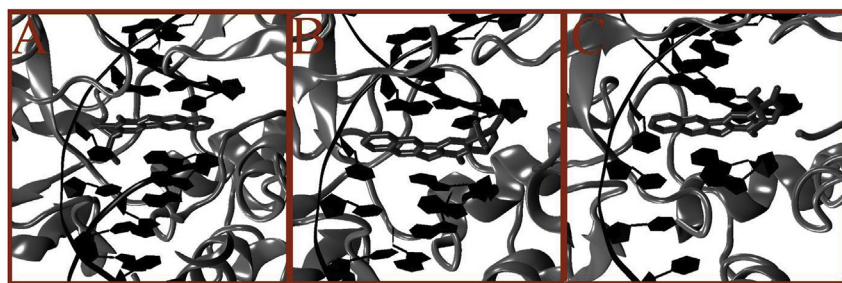
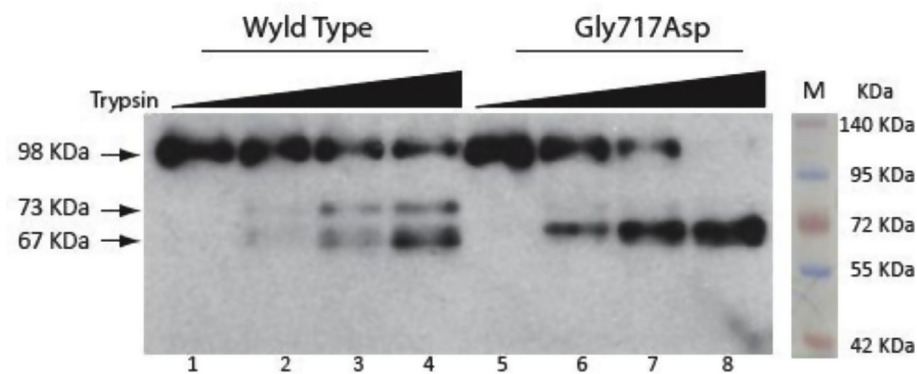


Fig. 6. Limited trypsin digestion. Full-length wild-type (lanes 1–4) or Gly717Asp mutant (lane 5–8) hTop1 was digested for 30 min at 37 °C with increasing concentrations of trypsin. The digestion products were fractionated by SDS-PAGE and visualized by immunoblot. M represented the protein marker fractionated on the same gel, the size of each band is indicated at the right side.



disorder in the protein. In detail proteolysis digestion has been done by incubating hTop1 and Gly717Asp with an excess of trypsin and the reactions were run on SDS-PAGE (Fig. 6). The trypsin cleaves the wild-type protein into two fragments having a molecular weight of 67 and 73 KDa (Fig. 6, lanes 2–4), while the Gly717Asp mutant shows a single fragment of about 70 kDa (Fig. 6, lanes 6–8), indicating that the mutant

is not proteolyzed and the two proteins offer different regions to the trypsin proteolytic digestion.

4. Discussion

In this study effect of the Gly717Asp mutation on the structural,

dynamical and functional properties of the hTop1 were analyzed through the combined functional and computational approaches. A viability assay carried out on EKY3 yeast cells, indicates that the mutant and wild-type enzyme show the same CPT sensitivity (Fig. 1). The characterization of the different catalytic steps of the Gly717Asp mutant showed the same cleavage rate compare to the wild-type protein (Fig. 2) but different religation kinetics (Fig. 3). In detail the Gly717Asp is faster in religating the R11 oligonucleotide when compared to hTop1 but the mutant shows drug sensitivity upon the addition of CPT (Fig. 3). As we previously demonstrated a fast religation rate is, normally, associated by a drug resistance [19,23]. It is interesting to remark that the same residue changed in Phe (Gly717Phe) shows fast religation rate and CPT resistance [23]. Moreover mutation of Gly717, corresponding to Gly721 in yeast Top1, in Asp dramatically enhances Top1 sensitivity to CPT *in vivo*, decreases the cleavage rate and shows an identical religation rate [24], highlighting the crucial role of this residue in modulating the catalytic properties and the drug reactivity. At this point in the study we are facing contradictory results: a mutant with a high religation rate is not CPT resistant *in vivo* and *in vitro*. To understand this behaviour CPT dose-dependent and time course cleavage/religation equilibrium has been performed. In the dose-dependent experiment the CPT mutant cleavable complex formation is higher than that found for the wild-type protein (lanes 11–13 with lanes 5–7, Fig. 4A). The time course cleavage/religation assay, at a fixed CPT concentration of 100 μM , indicates that the release of the drug is slower in the mutant than in the wild type (compare lanes 14–19 with lanes 5–10, Fig. 4B), suggesting that the drug persists in the mutant cleavable complex for a longer time than the wild type.

Using as receptor the structures obtained after 75 ns simulation of the wild-type and mutant covalent complex, the docking experiment has been performed, demonstrating that the mutant displays a slightly lower CPT binding energy than the wild-type. The main difference however, regards the orientation of the drug into the binding pocket, which allows a stronger interaction of CPT with the protein, and the presence of a unique binding mode in the mutant respect to the wild type (Fig. 5). This result suggests that the mutation is able to modify the architecture of the binding site increasing the persistence of the drug for the binding pocket. Moreover the occurrence of a different proteolysis pattern, from the limited proteolysis digestion (Fig. 6), suggests the presence of a conformational change induced by the mutation. The Gly717 is present on the loop at the border between helix 19 (the second helix of the linker domain), and helix 20 (the first helix of the C-terminal domain), harbouring the active site Tyr723. These results partially confirmed the findings of Bjornsti et al. in which the Gly721Asp in yeast Top1 dramatically enhances Top1 sensitivity to CPT. It has been also previously reported that the Gly717Phe mutant is CPT resistant due to a fast religation rate likely correlated to a different orientation of the linker domain and slight rearrangement of the active site as observed by *in silico* analysis [23]. Studies show that indeed in the presence of topotecan (TPT), the linker domain is less flexible and also, the Gly717 become part of the helix as seen by comparing the crystal structures of the protein in the presence and absence of TPT [29]. Analysis of the number of residues present in the helix 20 shows that in the case of wild-type protein the helix spans along the entire trajectory between residues Thr718 and Tyr723 (Suppl Fig. S1) while in the mutant the helix also contained Asp717 and Leu716 (Suppl. Fig. S1) making the helix two residues longer as observed in the ternary hTop1B-DNA-TPT complex [29]. The inclusion of the residue at position 717 in the helix when mutated to aspartic acid can be a direct result of the introduction of a negative charge in that particular position. Asp 717 was observed to establish a salt bridge with Lys720 present in the helix 20 for 77% of the simulation time, this interaction constraint at the position Asp717 enabling it to be included in the helix. Due to the formation of such structure and the occurrence of the Asp717-Lys720 can mask the lysine making it inaccessible for trypsin digestion. Taken together all these findings suggest the importance of position 717 in

enzyme modulation and catalysis particularly the religation step and CPT sensitivity.

Conflicts of interest

None declared.

Acknowledgments

We thank Dr. B. Morozzo Della Rocca for proof reading of the article and Dr. F. Iacovelli for helping in the computational analysis and graphical abstract.

Appendix A. Supplementary data

Supplementary data to this article can be found online at <https://doi.org/10.1016/j.abb.2019.01.007>.

References

- [1] J.C. Wang, Cellular roles of DNA topoisomerases: a molecular perspective, *Nat. Rev. Mol. Cell Biol.* 3 (2002) 430–440.
- [2] J.J. Champoux, DNA topoisomerases: structure, function, and mechanism, *Annu. Rev. Biochem.* 70 (2001) 369–413.
- [3] G. Chillemi, M. Redinbo, A. Bruxelles, A. Desideri, Role of the linker domain and the 203–214 N-terminal residues in the human topoisomerase I DNA complex dynamics, *Biophys. J.* 87 (2004) 4087–4097.
- [4] C. Losasso, E. Cretaio, K. Palle, L. Pattarello, M.-A. Bjornsti, P. Benedetti, Alterations in linker flexibility suppress DNA topoisomerase I mutant-induced cell lethality, *J. Biol. Chem.* 282 (2007) 9855–9864.
- [5] L. Stewart, G.C. Ireton, J.J. Champoux, The domain organization of human topoisomerase I, *J. Biol. Chem.* 271 (1996) 7602–7608.
- [6] M.R. Redinbo, J.J. Champoux, W.G. Hol, Novel insights into catalytic mechanism from a crystal structure of human topoisomerase I in complex with DNA, *Biochemistry* 39 (2000) 6832–6840.
- [7] M.R. Redinbo, L. Stewart, P. Kuhn, J.J. Champoux, W.G. Hol, Crystal structures of human topoisomerase I in covalent and noncovalent complexes with DNA, *Science* 279 (1998) 1504–1513.
- [8] M.R. Redinbo, L. Stewart, J.J. Champoux, W.G. Hol, Structural flexibility in human topoisomerase I revealed in multiple non-isomorphous crystal structures, *J. Mol. Biol.* 292 (1999) 685–696.
- [9] L. Stewart, A model for the mechanism of human topoisomerase I, *Science* 279 (1998) 1534–1541 (80-).
- [10] L. Stewart, G.C. Ireton, J.J. Champoux, Reconstitution of human topoisomerase I by fragment complementation, *J. Mol. Biol.* 269 (1997) 355–372.
- [11] J.J. Champoux, DNA topology and its biological effects, *Cold Spring Harb, 1990*, pp. 217–224.
- [12] Y. Pommier, *DNA Topoisomerases and Cancer*, Humana Press, 2012.
- [13] Y. Pommier, P. Pourquier, Y. Urasaki, J. Wu, G.S. Laco, Topoisomerase I inhibitors: selectivity and cellular resistance, *Drug Resist. Updates* 2 (1999) 307–318.
- [14] Y. Pommier, *Camptothecin in Cancer Therapy*, Humana Press, 2005.
- [15] Y. Pommier, Topoisomerase I inhibitors: camptothecins and beyond, *Nat. Rev. Canc.* 6 (2006) 789–802.
- [16] B.L. Staker, K. Hjerrild, M.D. Feese, C. a Behnke, A.B. Burgin, L. Stewart, The mechanism of topoisomerase I poisoning by a camptothecin analog, *Proc. Natl. Acad. Sci. U.S.A.* 99 (2002) 15387–15392.
- [17] S. Castelli, A. Coletta, I. D'Annese, P. Fiorani, C. Tesaro, A. Desideri, Interaction between natural compounds and human topoisomerase I, *Biol. Chem.* 393 (2012) 1327–1340.
- [18] J.E. Chrencik, B.L. Staker, A.B. Burgin, P. Pourquier, Y. Pommier, L. Stewart, M.R. Redinbo, Mechanisms of camptothecin resistance by human topoisomerase I mutations, *J. Mol. Biol.* 339 (2004) 773–784.
- [19] P. Fiorani, A. Bruxelles, M. Falconi, G. Chillemi, A. Desideri, P. Benedetti, A Single mutation in the linker domain confers protein flexibility and camptothecin resistance to human topoisomerase I, *J. Biol. Chem.* 278 (2003) 43268–43275.
- [20] I. D'Annese, C. Tesaro, P. Fiorani, G. Chillemi, S. Castelli, O. Vassallo, G. Capranico, A. Desideri, Role of flexibility in protein-DNA-drug recognition: the case of Asp677Gly-Val703Ile topoisomerase mutant hypersensitive to camptothecin, *J. Amino Acids* 2012 (2012) 206083.
- [21] P. Fiorani, C. Tesaro, G. Mancini, G. Chillemi, I. D'Annese, G. Graziani, L. Tentori, A. Muzi, A. Desideri, Evidence of the crucial role of the linker domain on the catalytic activity of human topoisomerase I by experimental and simulative characterization of the Lys681Ala mutant, *Nucleic Acids Res.* 37 (2009) 6849–6858.
- [22] C. Tesaro, B. Morozzo della Rocca, A. Ottaviani, A. Coletta, L. Zuccaro, B. Arnò, I. D'Annese, P. Fiorani, A. Desideri, Molecular mechanism of the camptothecin resistance of Glu710Gly topoisomerase IB mutant analyzed *in vitro* and *in silico*, *Mol. Canc.* 12 (2013) 100.
- [23] Z. Wang, I. D'Annese, C. Tesaro, S. Croce, A. Ottaviani, P. Fiorani, A. Desideri, Mutation of Gly717Phe in human topoisomerase 1B has an effect on enzymatic function, reactivity to the camptothecin anticancer drug and on the linker domain

- orientation, *Biochim. Biophys. Acta* 1854 (2015) 860–868.
- [24] M. van der Merwe, M.-A. Bjornsti, Mutation of Gly721 alters DNA topoisomerase I active site architecture and sensitivity to camptothecin, *J. Biol. Chem.* 6 (2008) 3305–3315.
- [25] C.M. Wright, M. van der Merwe, A.H. DeBrot, M.-A. Bjornsti, DNA topoisomerase I domain interactions impact enzyme activity and sensitivity to camptothecin, *J. Biol. Chem.* 290 (2015) 12068–12078.
- [26] M.A. Bjornsti, P. Benedetti, G.A. Viglianti, J.C. Wang, Expression of human DNA topoisomerase I in yeast cells lacking yeast DNA topoisomerase I: restoration of sensitivity of the cells to the antitumor drug camptothecin, *Cancer Res.* 49 (1989) 6318–6323.
- [27] I. D'Annessa, C. Tesauero, Z. Wang, B. Arnò, L. Zuccaro, P. Fiorani, A. Desideri, The human topoisomerase 1B Arg634Ala mutation results in camptothecin resistance and loss of inter-domain motion correlation, *Biochim. Biophys. Acta* 1834 (2013) 2712–2721.
- [28] B. Arnò, I. D'Annessa, C. Tesauero, L. Zuccaro, A. Ottaviani, B. Knudsen, P. Fiorani, A. Desideri, Replacement of the human topoisomerase linker domain with the plasmodial counterpart renders the enzyme camptothecin resistant, *PLoS One* 8 (2013) e68404.
- [29] G. Mancini, I. D'Annessa, A. Coletta, N. Sanna, G. Chillemi, A. Desideri, Structural and dynamical effects induced by the anticancer drug topotecan on the human topoisomerase I - DNA complex, *PLoS One* 5 (6) (2010 Jun 3) e10934.
- [30] B. Hess, C. Kutzner, D. van der Spoel, E. Lindahl, GROMACS 4: algorithms for highly efficient, load-balanced, and scalable molecular simulation, *J. Chem. Theor. Comput.* 4 (3) (2008 Mar) 435–447.
- [31] T. Darden, D. York, L. Pedersen, Particle mesh Ewald: an N [center-dot] log(N) method for Ewald sums in large systems, *J. Chem. Phys.* 98 (1993) 10089–10092.
- [32] B. Hess, H. Bekker, H. Berendsen, J. Fraaije, LINCS: a linear constraint solver for molecular simulations, *J. Comput. Chem.* 18 (1997) 1463–1472.
- [33] M. Parrinello, A. Rahman, Polymorphic transitions in single crystals: a new molecular dynamics method, *J. Appl. Phys.* 52 (1981) 7182–7190.
- [34] G.M. Morris, R. Huey, W. Lindstrom, M.F. Sanner, R.K. Belew, D.S. Goodsell, A.J. Olson, *J. Comput. Chem.* 30 (2009) 2785–2791.
- [35] G.M. Morris, D.S. Goodsell, R.S. Halliday, R. Huey, W.E. Hart, R.K. Belew, A.J. Olson, *J. Comput. Chem.* 19 (1998) 1639–1662.